HHS Public Access

Author manuscript

Exp Neurol. Author manuscript; available in PMC 2019 May 02.

Published in final edited form as:

Exp Neurol. 2018 February ; 300: 121–134. doi:10.1016/j.expneurol.2017.11.001.

Newfound sex differences in axonal structure underlie differential outcomes from in vitro traumatic axonal injury

Jean-Pierre Dollé[a], **Andrew Jaye**[a], **Stewart A. Anderson**[b], **Hossein Ahmadzadeh**[c], **Vivek B. Shenoy**[c], and **Douglas H. Smith**[d,*]

[a]Penn Center for Brain Injury and Repair, Department of Neurosurgery, University of Pennsylvania, 220 South 33rd Street, 283 Towne Building, Philadelphia, PA 19104, USA

[b]Department of Psychiatry, Children's Hospital of Philadelphia, Philadelphia, PA 19104, USA

[c]Department of Materials Science and Engineering, 3231 Walnut Street, Room 309, The Laboratory for Research on the Structure of Matter, University of Pennsylvania, Philadelphia, PA 19104, USA

[d]Penn Center for Brain Injury and Repair, Department of Neurosurgery, University of Pennsylvania, 3320 Smith Walk Hayden Hall 105, Philadelphia, PA 19104, USA

Abstract

Since traumatic axonal injury (TAI) is implicated as a prominent pathology of concussion, we examined potential sex differences in axon structure and responses to TAI. Rat and human neurons were used to develop micro-patterned axon tracts in vitro that were genetically either male or female. Ultrastructural analysis revealed for the first time that female axons were consistently smaller with fewer microtubules than male axons. Computational modeling of TAI showed that these structural differences place microtubules in female axons at greater risk of failure during trauma under the same applied loads than in male axons. Likewise, in an in vitro model of TAI, dynamic stretch-injury to axon tracts induced greater pathophysiology of female axons than male axons, including more extensive undulation formations resulting from mechanical breaking of microtubules, and greater calcium influx shortly after the same level of injury. At 24 h post-injury, female axons exhibited significantly more swellings and greater loss of calcium signaling function than male axons. Accordingly, sexual dimorphism of axon structure in the brain may also contribute to more extensive axonal pathology in females compared to males exposed to the same mechanical injury.

Keywords

Sexual dimorphism; Traumatic axonal injury; Undulations; Calcium; Axon diameter; Microtubules

*Corresponding author. smithdou@pennmedicine.upenn.edu.

Author contributions

J-P.D, A.J, D.H.S designed and performed in vitro experiments. H.A, V.B.S, D.H.S developed the mathematical model. S.A.A assisted with human cell biology and provided human differentiated iPSCs. J-P.D, H.A, V.B.S, D.H.S wrote the manuscript.

Conflicts of interest

None.

1. Introduction

While the underlying causes of concussion symptoms have yet to be fully characterized, traumatic axonal injury (TAI) has emerged as a primary neuropathological signature (Johnson et al. 2013). This likely reflects the unique vulnerability of axons to mechanical damage as the brain undergoes high rotational accelerations. In particular, it has been previously demonstrated that at the moment of trauma, axonal microtubules can mechanically break, leading to undulations along the length of the axons, interruption of axonal transport and accumulation of transported proteins in varicose swellings, characteristic of TAI pathology (Smith et al. 1999; Tang-Schomer et al. 2012; Tang-Schomer et al. 2010). In parallel, injured axons may undergo massive influx of sodium and calcium ions, which disrupts signaling and activates proteases that can lead to depolymerization of the axonal cytoskeleton (Iwata et al. 2004; Wolf et al. 2001). These pathological changes can ultimately lead to secondary axon disconnection and degeneration. However, there is a large range of these responses, even for axons in the same tract receiving the same injury. This suggests that potential differences in morphology such as size predispose some axons to be more susceptible to mechanical damage.

MRI studies show larger white matter volumes in males than females (Gur et al. 1999) with the extent of myelination appearing to remain constant for females and decreasing in males (Paus and Toro 2009; Perrin et al. 2009) suggesting axons in male brains to be larger on average than those in female brains. Alexander and colleagues show, using diffusion MRI, that at various positions along the corpus collosum, female mean axonal diameters are smaller than males (Alexander et al. 2010). Using electron microscopy, differences in axonal diameter have been observed in the rat corpus callosum (Mack et al. 1995; Pesaresi et al. 2015). This raises the intriguing possibility that sex-based differences in average axon size could represent differences in the mechanical vulnerability of axons exposed to dynamic forces during concussion.

Notably, males represent a high majority of emergency department visits for sports- and recreation-related concussion (Gaw and Zonfrillo 2016), attributed primarily to their greater exposure to activities with a risk of head impacts compared to females. However, it has recently been observed that female athletes have a higher rate of concussion (Abrahams et al. 2014; Covassin et al. 2003; Marar et al. 2012) and appear to have worse outcomes than their male counterparts participating in the same sport (Bazarian and Atabaki 2001; Broshek et al. 2005). While the comparative impact forces are not known, the differences in incidence and outcome suggest that there was greater damage to female brains.

Here, we examined potential sex-associated differences in axon structure and response to TAI. Specifically, we performed transmission electron microscopy (TEM) assessment of micropatterned female and male axons from both primary rat cortical neurons and differentiated human induced pluripotent stem cell (iPSC) neurons to determine potential sex differences in axon ultrastructure. We then evaluated sex-associated differences in the axonal response to dynamic stretch injury using established computational and in vitro models of TAI.

2. Materials and methods

2.1. Axonal tracts using micro-patterned channels

2.1.1. Rat axonal cultures—To create parallel lanes of axon fascicles spanning populations of neurons, a culture system was used as previously described in detail (Tang-Schomer et al. 2010). Briefly, a molded elastomeric stamp with lithographically-fabricated micro-channels was placed against a deformable silicone membrane (0.002-in. thickness, Specialty Manufacturing) (Fig. 1a). The channels (0.2 mm width × 2 mm length × 0.2 mm height) were pre-coated with 0.5 mg/ml polyethylenimine (Sigma-Aldrich) and 5μg/cm^2 laminin (BD Biosciences) to allow for axon-only longitudinal outgrowth to occur and functional connections to be made between the two cell populations.

All animal procedures were performed in accordance with the National Institutes of Health guide for the care and use of Laboratory animals and protocols were approved by the Institutional Animal Care and Use Committee (IACUC) at the University of Pennsylvania. Primary cortical neurons from male and female embryonic day 18 (E18) Sprague-Dawley pups (Charles River) were dissociated and plated at a density of 300,000 cells/ml on our deformable membrane. Male pups were identified by the presence of striated testes found just below the kidneys (Fairbanks et al. 2013). Female pups were identified by the lack of testes and the presence of ovaries. Pup sex was confirmed by performing polymerase chain reaction (PCR) analysis for the male-specific gene SRY, with SRY not being observed in female pups.

Cells were plated and cultured in NeuroBasal medium (Invitrogen) supplemented with 2% B-27 neural supplement (Invitrogen), 400 μM L-glutamine (GlutaMAX, Invitrogen), 1% penicillin/streptomycin (P/S) and 5% fetal bovine serum (FBS, HyClone). Twenty-four hours after initial plating, the micropatterned stamps were removed and the complete media was exchanged with P/S and FBS free media. Specifically, axonal processes started to enter the micro-channels within 3–4 days in culture. By 7–10 days in vitro, axons had traversed the channels to synapse with neuronal somata on the opposite side of the 2 mm long channels. A clear ‘axon-only’ region was thus defined between the independent neuronal populations, as shown previously Fig. 1a) (Tang-Schomer et al. 2010). Cultures were maintained for approximately 12–14 days before being injured or processed for transmission electron microscopy.

2.1.2. Human axonal cultures—We pursued multiple sources to acquire female and male differentiated human induced pluripotent stem cell (iPSC) lines obtained from healthy individuals (Table 1). These lines were differentiated into neurons by either overexpression of Neurogenin-2 (Ngn2) (Zhang et al. 2013) or lack of morphogens (Espuny-Camacho et al. 2013) (generously donated by Dr. Isaac Chen of the Department of Neurosurgery, University of Pennsylvania). The lines used for Ngn2 overexpression were generated by the laboratory of Dr. Herbert Lachman using episomal plasmid based vectors (Lin et al. 2016; Pedrosa et al. 2011). Lines were confirmed for sex and absence of major CNVs by MLPA testing (Vorstman et al. 2006). Differentiated iPSCs were plated on our micropatterned deformable membranes allowing for separation of cell soma region and creating an axon-only region. These iPSCs were cultured in Neurobasal medium (Invitrogen) supplemented with 2% B-27

neural supplement (Invitrogen), 10 ng/ml brain derived neurotrophic factor (BDNF – Sigma-Aldrich), 10 ng/ml Neurotrophin-3 (Peprotech), 2μg/ml doxycycline (Sigma-Aldrich), 6 mg/ml glucose (Sigma-Aldrich) and 2 mM glutamax (Invitrogen). Prior to plating, the silicone membranes were precoated with 5% matrigel (Sigma-Aldrich). Differentiated iPSCs were plated at a density of 200,000–800,000 cells/ml. Media was changed every three to four days, with 10μg/ml AraC added to cultures on Day 4. Cultures were maintained for approximately 17–19 days before being injured or processed for transmission electron microscopy.

All cells were manipulated and cultured in a sterile environment using good cell culture practice and routinely tested for mycoplasma using standard methods.

2.2. Transmission electron microscopy (TEM)

Uninjured control axons were fixed and processed for analysis using TEM. For each experimental condition, 4 independent cultures were processed. Specifically, cells were fixed with a mixture of 2% paraformaldehyde (Electron Microscopy Sciences) and 2.5% glutaraldehyde (Sigma-Aldrich) overnight. After washing with 0.1 M sodium cacodylate buffer (3 × 10 min), cells were post-fixed with osmium (2%) plus potassium ferricyanide (1.5%), followed with three buffer washes and two diH_2O washes. To enhance the intensity of cell membranes, cells were stained with 2% uranyl acetate for 20 min, followed again with two diH_2O washes. Serial dehydration was performed via 3 min incubations in 50%–100% EtOH. Post-fixed cultures were embedded in resin in situ, separated from the silicone membrane, and re-embedded.

A ~1 mm × 1 mm × 60 nm thickness region perpendicular to the middle of the axon-only region was cut. Axons were selected based on: the axolemma should be intact, no organelles should be present, and microtubules should be cross-sectionally cut (should have a round morphology). Axon area was measured using ImageJ (NIH, USA). Image analysis with respect to axon area and microtubule number was confirmed by blinded analysis.

2.3. Mathematical model of axonal stretch injury

We used an established mathematical model of dynamic TAI (Ahmadzadeh et al. 2014, 2015) that previously demonstrated the viscoelastic response that results in immediate microutbule breakage due to axon stretch injury. Here, we set the axon geometry in the model to reflect the sex differences in axon diameter and microtubule number that was determined from the TEM analyses.

In this model, the axon is represented by a two-dimensional flattened layout of a longitudinal section through the axon (Fig. 2a). The axon cytoskeleton model consists of a staggered array of parallel microtubules (with length L=100μm, outer and inner radii R_O=12.5 nm and R_I=7 nm and elastic modulus E_m=1.9 GPa) (Lu et al., 2016), cross-linked by inverted pairs of tau proteins spaced at a distance d_T=30 nm (Fig. 2a). The cross-linker proteins are modeled using viscoelastic elements i.e. with a spring and a dashpot placed in parallel (Fig. 2b). The spring (with stiffness K=0.05 pN/nm) (Sendek et al., 2014) represents the backbone stiffness of the cross-linker protein and the dashpot (with a relaxation time-scale η=0.35 sec) (Suresh, 2007) represents the stiffness that arises from its intra-molecular

bonds at fast loading rates. In the present study, the model was modified to represent the relative difference in number of microtubules within smaller diameter (5 microtubules) and larger diameter (9 microtubules) rat cortical axons. (Fig. 2a).

As axons are loaded, mechanical forces are transmitted between neighboring microtubules through stretching of the cross-linker proteins, resulting in the sliding of microtubules. By defining the longitudinal displacements for the microtubules ($u_i(x)$ where i denotes the microtubule labels as shown in Fig. 2b), we can write the force-balance equations as (Eq. (1)):

For smaller axons with fewer microtubules:

$$-L_c^2\frac{\partial^2 u_i(x,t)}{\partial x^2} = \eta\left(\frac{\partial u_i(x,t)}{\partial t} - \frac{\partial u_{i-1}(x,t)}{\partial t} + \frac{\partial u_i(x,t)}{\partial t} - \frac{\partial u_{i+1}(x,t)}{\partial t}\right)$$

$$+ u_i(x,t) - u_{i-1}(x,t) + u_i(x,t) - u_{i+1}(x,t) \quad i = 2,\ 4$$

$$L_c^2\frac{\partial^2 u_i(x,t)}{\partial x^2} = \eta\left(\frac{\partial u_i(x,t)}{\partial t} - \frac{\partial u_{i-1}(x,t)}{\partial t} + \frac{\partial u_i(x,t)}{\partial t} - \frac{\partial u_{i+1}(x,t)}{\partial t}\right)$$

$$+ u_i(x,t) - u_{i-1}(x,t) + u_i(x,t) - u_{i+1}(x,t) \quad i = 3$$

For larger axons with more microtubules:

$$-L_c^2\frac{\partial^2 u_i(x,t)}{\partial x^2} = \eta\left(\frac{\partial u_i(x,t)}{\partial t} - \frac{\partial u_{i-1}(x,t)}{\partial t} + \frac{\partial u_i(x,t)}{\partial t} - \frac{\partial u_{i+1}(x,t)}{\partial t}\right) \qquad (1)$$

$$+ u_i(x,t) - u_{i-1}(x,t) + u_i(x,t) - u_{i+1}(x,t) \quad i$$

$$= 2,\ 4,\ 6,\ 8$$

$$L_c^2\frac{\partial^2 u_i(x,t)}{\partial x^2} = \eta\left(\frac{\partial u_i(x,t)}{\partial t} - \frac{\partial u_{i-1}(x,t)}{\partial t} + \frac{\partial u_i(x,t)}{\partial t} - \frac{\partial u_{i+1}(x,t)}{\partial t}\right)$$

$$+ u_i(x,t) - u_{i-1}(x,t) + u_i(x,t) - u_{i+1}(x,t) \quad i = 3,\ 5,\ 7$$

where L_c represents the length over which the longitudinal forces are transmitted between neighboring microtubules and is given by (Eq. (2)):

$$L_c = \frac{\pi\left(R_O^2 - R_I^2\right)d_T E_m}{6\,K} \approx 8\mu \qquad (2)$$

Here, we also accounted for differences in the surface to volume ratios of larger axons with more microtubules vs. smaller axons with fewer microtubules relative to microtubule

attachments to the axolemma. As has been previously demonstrated, microtubules adjacent to the membrane are anchored to actin filaments by microtubule/actin binding proteins (Wegmann et al., 2011). We modeled these connections using a viscoelastic element, composed of a spring and a dashpot placed in parallel (Fig. 2b). In order to ensure that the microtubule bundle is able to slide with respect to the axolemma in response to longitudinal strains, it was assumed that the microtubule/actin connections were weaker than the cross-linker/cross-linker connections. The spring stiffness for the microtubule/actin binding was assumed to be (K_a=0.01K) and for simplicity, its relaxation time is equal to the cross-linking protein relaxation time-scale (η=0.35 sec).

The force-balance equations for microtubules located at the periphery of the axon are (Eq. (3)):

For smaller axons with fewer microtubules:

$$L_c^2\frac{\partial^2 u_1(x,t)}{\partial x^2} = \eta\left(\frac{\partial u_1(x,t)}{\partial t} - \frac{\partial u_2(x,t)}{\partial t}\right) + u_1(x,t) - u_2(x,t) + \frac{K_a^2}{K^2}\left(\eta\frac{\partial u_1(x,t)}{\partial t} + u_1(x,t)\right)$$

$$L_c^2\frac{\partial^2 u_5(x,t)}{\partial x^2} = \eta\left(\frac{\partial u_5(x,t)}{\partial t} - \frac{\partial u_4(x,t)}{\partial t}\right) + u_5(x,t) - u_4(x,t) + \frac{K_a^2}{K^2}\left(\eta\frac{\partial u_5(x,t)}{\partial t} + u_4(x,t)\right)$$

For larger axons with more microtubules:

$$L_c^2\frac{\partial^2 u_1(x,t)}{\partial x^2} = \eta\left(\frac{\partial u_1(x,t)}{\partial t} - \frac{\partial u_2(x,t)}{\partial t}\right) + u_1(x,t) - u_2(x,t) + \frac{K_a^2}{K^2}\left(\eta\frac{\partial u_1(x,t)}{\partial t} + u_1(x,t)\right) \quad (3)$$

$$L_c^2\frac{\partial^2 u_9(x,t)}{\partial x^2} = \eta\left(\frac{\partial u_9(x,t)}{\partial t} - \frac{\partial u_8(x,t)}{\partial t}\right) + u_9(x,t) - u_8(x,t) + \frac{K_a^2}{K^2}\left(\eta\frac{\partial u_9(x,t)}{\partial t} + u_9(x,t)\right)$$

In order to obtain the mechanical forces acting on the microtubules during injury, we specify the displacement at one end of the microtubules as:

For smaller axons with fewer microtubules:

$$u_2\left(\frac{L}{2},t\right) = u_4\left(\frac{L}{2},t\right) = \dot{\varepsilon}tL$$

For larger axons with more microtubules:

$$u_2\left(\frac{L}{2},t\right)=u_4\left(\frac{L}{2},t\right)=u_6\left(\frac{L}{2},t\right)=u_8\left(\frac{L}{2},t\right)=\dot{\varepsilon}tL \quad (4)$$

where $\dot{\varepsilon}$ is the strain rate and $\dot{\varepsilon}t$ is the applied strain. Here we have assumed a reference coordinate system placed at the center of the microtubules, in such a way that the x-axis is oriented along the length of the microtubules.

2.4. In vitro dynamic stretch injury of axons

Axonal stretch injury was performed using the established model, as described previously in detail (Iwata et al. 2004; Tang-Schomer et al. 2010; Wolf et al. 2001). Notably, this model examines the response of unmyelinated axons to dynamic injury based on previous observations that approximately 50% of axons in many white matter tracts are unmyelinated (Ozdogmus et al. 2009; Swadlow et al. 1980) and that these unmyelinated axons appear to be the more vulnerable to become damaged or dysfunctional following traumatic injury compared to myelinated axons (Reeves et al. 2005; Reeves et al. 2012; Staal and Vickers 2011).

Experiments using rat cortical cells were performed at 12–14 days in vitro and those using differentiated human iPSCs were performed at 17–19 days in vitro. Notably, this is the first study to use human iPSC neurons in the axon stretch injury model. Culture wells were placed in a sealed, pressure controlled, device at an orientation aligning the region of cultured axons directly above a machined 2 × 15 mm slit in a metal plate (Fig. 1b, c). A controlled air pulse was then injected into the sealed pressure chamber subjecting axons to a strain rate of $1 \times 50\ S^{-1}$ (Tang-Schomer et al. 2010). This pressure change within the chamber results in the rapid downward deflection of the axon-only region of membrane through the slit positioned below (Fig. 1c). As such, only the axon-only region undergoes rapid stretch.

2.5. Axonal undulation calculation

We have shown previously that the immediate breaking of axonal microtubules during injury impedes relaxation to pre-stretch length, thereby causing an undulated appearance. Undulating axons were randomly chosen. To measure the increase in localized axon length per undulation, calcium fluorescence images were taken before injury and immediately following injury. The percentage increase in length was calculated by subtracting the axon length before injury from the length immediately following injury and dividing by the original axon length.

2.6. Intra-axonal calcium changes

Intra-axonal calcium was monitored using the genetic calcium indicator GCaMP6 (University of Pennsylvania, Vector Core). Rat cells were transduced with GCaMP6 on day 5 for 24 h and differentiated human iPSCs for 90 h. Baseline fluorescence and changes in calcium concentrations were monitored before injury, and 5mins, 10mins, 15mins following injury. A potential caveat to the in vitro model is axon-to-axon connections which may affect

fluorescence analysis. In order to minimize potential differences in numbers of axons analyzed (although these axonal aggregates appear to be similar in geometry between male and female cultures), uniform thickness and length regions of interest were selected across the width of the axon lane. At least four different regions of interest were selected outside of the axon lane, which represented background fluorescence values that were averaged, subtracted from the axonal regions of interest and the resulting fluorescence intensity normalized to intensity before injury. Data collection and analysis were performed by different experimenters yielding similar results.

2.7. Axonal transport interruption

Intra-axonal beta-tubulin accumulation has previously been shown to represent regions of axon transport interruption (Tang-Schomer et al. 2012). Female and male rat cortical uninjured control and 24 h following stretch injury axon tracts, were fixed with 2% paraformaldehyde (Electron Microscopy Sciences) and 0.1% glutaraldehyde (Sigma-Aldrich) and immunostained with the primary antibody for beta-tubulin (Sigma-Aldrich, T8578, 1:500, RRID:AB_1841228) and Alexa Fluor 647 (Invitrogen, A31571, 1:500) secondary antibody.

2.8. Measuring functional intra-axonal calcium signaling

In order to assess the number of axons that were capable of transmitting calcium signals 24 h following stretch injury, female and male rat cortical axons were monitored using GCaMP6. These GCaMP6 positive axons were compared to the total number of axons in the same axon tract (which was confirmed by immunostaining for Tau (Dako, A0024)). Injured axon tracts were compared to uninjured control axon tracts.

2.9. Statistical analyses

Values are expressed as mean ± standard error of the mean (s.e.m). Statistical significance was evaluated using unpaired students *t*-test and $P < 0.05$ was considered significant.

3. Results

3.1. Transmission electron microscopic images reveal sex differences in in vitro cultured rat and human axon ultrastructure

Since axonal damage is thought to be a predominant neuropathology of concussion (Benson et al. 2007; Blumbergs et al. 1994; Johnson et al. 2013; Smith et al. 2013; Yuh et al. 2013), we investigated potential sex-based differences between male and female axons at the structural and ultra-structural levels as well as examining how potential structural differences could affect outcome from TAI. As previously described, micropatterned parallel arrangements of 2 mm long axononly tracts were created in vitro from rat cortical neurons, designed to mimic the geometry of axon tracts spanning two populations of neurons in the brain (Fig. 1a). In addition, to corroborate potential clinical relevance of axon cultures from rat neurons, the first micropatterning of axon tracts derived from differentiated human induced pluripotent stem cells (iPSC) was performed. The neuron sources for each culture were isolated from either female or male sources based on genetic testing. Transmission electron microscopy (TEM) was used to examine cross sections from the middle of the

micropatterned axon fascicles. This revealed a fundamental sex-based difference from the entire axon girth down to nanoscale features. Specifically, male rat axons were found to have approximately 61% larger cross-sectional areas (43,140nm^2 vs. 26,756nm^2) with a 62% increase in number of microtubules per axon as compared to female rat axons (9.4 vs. 5.8) (Fig. 3a–d). Similarly for human axons, male axons showed an approximately 80% increase in cross-sectional area (91,913nm^2 vs. 50,981nm^2) and a 55% increase in number of microtubules per axon as compared to female axons (11.8 vs. 8.2) (Fig. 3e–h). Interestingly, microtubule density was significantly different for only human but not rat axons. Overall, human axons were found to be larger than rat axons.

For both species, we did not observe a sex based difference in the extent of fasciculation formation in the micropatterened lanes. In addition, there did not appear to be an overt difference in the diameter of axons in smaller fascicles compared to those in larger fascicles.

3.2. Mathematical model of axonal stretch injury confirms smaller axons are more susceptible to microtubule rupture than larger axons

We applied the same sex differences in axonal architecture derived from the TEM data, to investigate if smaller axons with fewer microtubules would be more vulnerable to rupture following axonal trauma. We used an established mathematical model paradigm, to generate representative smaller diameter axons with less microtubules or larger diameter axons with more microtubules. The model includes viscoelastic elements of proteins crosslinking microtubules throughout the axons and actin filaments binding microtubules near the periphery (Fig. 4a).

Using dynamic loading rates of axons relevant to TBI (i.e. a strain rate of $1 \times 50\ S^{-1}$), and specifying a microtubule strain threshold (Ahmadzadeh et al. 2014; Janmey et al. 1991), the model was used to identify thresholds of strain and strain rates that result in the rupture of microtubules. It was found that in response to the same level of dynamic stretch, microtubule strain is higher in smaller diameter axons with fewer microtubules than in larger diameter axons with more microtubules (Fig. 4b). Microtubule strain was calculated as a function of the applied stain rate (Fig. 4c), while the overall level of the microtubule strain increases with increased strain-rate, microtubules in smaller diameter axons experience larger strains compared to microtubules in larger diameter axons. Using a microtubule strain threshold, the model shows: 1) microtubules in smaller diameter axons fail at lower strain-rates than those in larger diameter axons (Fig. 4c) and, 2) employing the same applied strain rate, smaller diameter axons with fewer microtubules fail at a lower applied stretch than larger diameter axons with more microtubules (Fig. 4d).

3.3. Rat and human axons display sex differences in axonal undulations following in vitro traumatic axonal injury

Progressing from the mathematical model to a well-characterized in vitro model of traumatic axonal injury, we examined potential sex-based differences in the vulnerability of genetically “female” axons compared to “male” axons to mechanical trauma. Notably, this model mimics the deformation biomechanics of unmyelinated axons during rotational acceleration in human TBI (Fig. 1c) and allows for examination of the immediate and

evolving effects of TAI following an injury that is applied exclusively to axons (Tang-Schomer et al. 2012; Tang-Schomer et al. 2010; Wolf et al. 2001; Yuen et al. 2009). As with the TEM studies, micropatterned parallel arrangements of 2 mm long axon-only tracts were created on flexible membranes, using both primary rat cortical neurons and differentiated human iPSC neurons, isolated from female or male sources. Dynamic uniaxial stretch injury isolated to the axonal tracts was induced at set levels using established parameters (Fig. 1c). Immediately after injury, axons display an undulated morphology, readily seen with light and fluorescent microscopy. Examining injured axons with TEM immediately after injury, mechanical breaking of axonal microtubules was observed within the undulations (red arrows, Fig. 5a). Notably, it has previously been noted that the broken microtubules impede relaxation of the axons to their pre-injury length, thereby causing the undulations (Fig. 5a, b, e), as has been previously observed acutely in both in vitro stretch injury (rat axons) and after TBI in humans (Tang-Schomer et al. 2012; TangSchomer et al. 2010). In this study, axons from both rat and human sources exhibited the characteristic undulated morphologies (Fig. 5b, e), Examining a potential sex difference in the extent of these immediate morphological changes, it was found that rat and human female axons displayed a greater number of undulations along the length of the axon as well as a localized increase in axon length per undulation, compared to male axons from corresponding sources (Fig. 5c, d and e). Notably, these are the first data generated using human iPSC neurons to examine TAI, supporting the clinical relevance of the similar findings using rat neurons.

3.4. Intra-axonal calcium influx following in vitro traumatic axonal injury shows sex differences

In addition to morphological changes, another major pathological feature of TAI is the aberrant influx of ions into the axon. In particular, excessive calcium influx can disrupt signaling and activate proteases leading to chemical damage to the axonal cytoskeleton. Since the level of intra-axonal calcium influx in the in vitro model is proportional to the applied injury, it can be used as a marker of injury severity (Yuen et al. 2009). In the present study, intra-axonal calcium concentrations were monitored by transducing neurons with the genetically encoded calcium indicator GCaMP6. Rat and human axon tracts were stretch-injured and calcium fluorescence detection demonstrated significant increases in intra-axonal calcium levels that persisted for at least 15 min (Fig. 6a). As previously described, within each tract, there was a wide range in the extent of calcium concentration increases in individual axons. In particular, axons with more extensive undulation formations post-injury were generally found to have higher calcium concentrations than nearby axons that maintained a more normal straight morphology. In concordance, female axons were uniformly accompanied by significantly greater calcium levels compared to male axons at all time points evaluated, from 1 min through 15 min following the same level of injury (Fig. 6b and c). Calcium influx immediately following injury is significantly greater in human axons than in rat axons, i.e. 2.5 vs. 1.8-fold.

3.5. Sex based differences in axon transport interruption and calcium signaling dysfunction following in vitro traumatic axonal injury

The primary mechanical injury and secondary chemical damage can work synergistically to disrupt axonal transport and push damaged axons towards degeneration, as previously

characterized (TangSchomer et al. 2012; Tang-Schomer et al. 2010). In the present study, female axons fared far worse than male axons with these deleterious processes than male axons exposed to the same level of injury. Specifically, immunocytochemical analyses demonstrated that the extent of accumulation of beta-tubulin in varicose axonal swellings along injured axons was much greater in female axons compared to male axons at 24 h after injury (Fig. 7a). Likewise, a greater reduction of axons that remained functional, as demonstrated by the capacity to propagate calcium signaling 24 h after trauma, was observed in female axon tracts compared to male axon tracts (Fig. 7b). This reduction in function was highlighted by immunostaining the same tract for tau to represent the total number of axons.

4. Discussion

Here, significant sexual dimorphism of axonal architecture for both rat and human neurons was observed. A newfound difference in microtubule number corresponding to overall size differences was shown to predispose female axons to greater mechanical damage and physiological dysfunction as shown with both computational modeling and an in vitro model of TAI. In particular, we found that while both female and male axons displayed immediate formation of undulations post-injury, female axons had substantially more undulations per axon length and their average undulation size was greater compared to male axons. In addition, female axons displayed greater post-traumatic calcium influx, axon transport interruption and degeneration compared to male axons receiving the same injury (Fig. 8).

It is certainly plausible that the sexual dimorphism of axon ultrastructure observed in vitro is also true for axons in the brain. Indeed, indirect evidence using human in vivo neuroimaging shows male white matter being proportionately larger than females (Gur et al. 1999), and that male myelination appears to decrease during adolescence while female myelination stays relatively constant, suggests axonal diameter plays a role. Direct evidence from EM analysis of the rat corpus callosum shows female axon diameters to be smaller than male axons (Mack et al. 1995; Pesaresi et al. 2015), which is corroborated by a newer diffusion MRI technique showing female mean axon diameters within the human corpus callosum to be smaller than male axons (Alexander et al. 2010), Interestingly, it has even been speculated that this size difference may be due to number of microtubules in male axons than female axons in the brain (Perrin et al. 2008). The current data provides the first direct in vitro evidence supporting this premise.

It has previously been thought that testosterone plays a main role in the development of larger axons for males since manipulation of testosterone exposure in rats had significant effects on axon size (Pesaresi et al. 2015). However, the absence of testosterone or other sex hormones in our in vitro preparations of neurons suggests that the observed sex differences in axon caliber and structure have another gene expression origin, likely from the Y chromosome, which would not require constant exposure to sex hormones. We cannot, however, rule out other potential influences, such as epigenetic changes, that may play a role in axon caliber for both rats and humans. Moreover, consistent with previous observations that axonal caliber increases with increasing brain size (Wang et al. 2008), we found that on

average, human axons were larger than rat axons, lending further support that as yet unknown factors dictate axon size beyond the influence of sex hormones.

Although the evolutionary foundation for the observed sex difference in axonal size is unknown, there may be a functional need to maintain a similar number of axons in a given tract for both sexes, with females having the challenge to accommodate this within a proportionately smaller brain (Dekaban 1978). An example of this may be the corpus callosum of humans, where the average axon diameter and total tract volume is greater for males, yet females actually have a higher total number of axons in this tract (Aboitiz et al. 1992). Alternatively, since primitive times, as males have preferentially engaged in activities with a risk of head trauma, there may have been an evolutionary advantage to maintain a more mechanically resilient axonal ultrastructure. Whatever the origin, it is interesting to consider that these sex differences are coming to light with the advent of an increasingly greater number of females exposed to TAI.

Should sexual dimorphism of axon ultrastructure be also conclusively demonstrated in the brain, the current in vitro findings may have implications for concussion, where axonal injury is the most commonly described pathological feature. It is conceivable that under the same level of mechanical loading during head impact, axons in female brains may be more susceptible to damage than axons in male brains due to fundamental differences in axon ultrastructure.

The current data provide a potential example of how the brain could literally break upon head impact. It has long been recognized that the viscoelastic nature of axons in the white matter renders them particularly vulnerable to damage at all severities of TBI. In particular, under dynamic loading of head impact, the stiffness of axons is thought to increase, thereby causing internal damage upon deformation. Using rat axons in an in vitro model of TAI, we recently demonstrated that axonal microtubules are the principal structural components that can physically break at the moment of trauma, resulting in sites of transport interruption at the level of individual microtubules (Tang-Schomer et al. 2012; Tang-Schomer et al. 2010). In addition, the broken microtubules were found to impede relaxation of the injured axons to their pre-stretch length, resulting in an undulated axon morphology that has also been observed in post-mortem evaluation of acute TBI tissue (Tang-Schomer et al. 2012; Tang-Schomer et al. 2010).

The underlying principles of the present study are based on our recent computational model that revealed the microtubule stabilizing protein tau is a key viscoelastic element underlying rate-dependent microtubule rupture in TAI. (Ahmadzadeh et al. 2014, 2015). Since stretching axons under normal conditions causes microtubules to slide past each other, crosslinking proteins maintain stabilization by progressively extending from their resting tertiary form through the breaking of weak molecular bonds. This allows the crosslinking proteins to maintain their attachments to the repositioned microtubules. However, under high strain rates, the crosslinking proteins behave stiffer since the molecular bonds cannot be released quickly enough. This transfers high stress onto the microtubule attachments that can result in mechanical rupture of some microtubules.

In the present study, mathematical modeling of TAI across a range of applied strain rates revealed microtubule rupture at lower levels in smaller axons with less microtubules compared to larger axons with more microtubules exposed to identical injury parameters. This was primarily attributed to differences in resistance of microtubule sliding during stretch. Specifically, with a smaller diameter and greater periphery to area ratio for smaller diameter axons, the peripheral forces of crosslinking proteins binding to microtubules were more dominant than for larger diameter axons. As such, under the same levels of axon stretch, there were higher longitudinal strains along microtubules in smaller diameter axons with less microtubules than in larger diameter axons with more microtubules, leading to greater mechanical failure of the microtubules. Microtubule length may have an effect on microtubule failure (Ahmadzadeh et al. 2014). However, to date there is no literature examining sex-based differences in microtubule length, and based on our own unpublished work examining longitudinal EM sections, we do not observe any distinct sex-based differences in microtubule length.

Future considerations to improve the mathematical model include the addition of other specific structural elements, in particular, neurofilaments (NFs). NFs have been shown to influence axonal diameter (Nixon et al. 1994), are found to be modified after TBI (Chen et al. 1999; Povlishock et al. 1997), and likely provide mechanical support to the axonal ultrastructure (Miyata et al. 1986; Yuan et al. 2017). However, due to their extremely small size, identification of neurofilament number and arrangement could not be accurately determined with EM analysis to be included in the current mathematical model. In addition, influence of connections between adjacent axons forming fascicles may also be considered for the model to examine how these mechanical influences affect responses to dynamic stretch injury.

The current mathematical model predictions were corroborated by the in vitro TAI data, which showed greater microtubule failure and correspondingly more undulations for female axons that have smaller cross sectional areas and fewer microtubules compared to male axons. This was consistent for both rat axons and the newly studied axon tracts micropatterned from human iPSC neurons. As the stiffest load bearing structures of the axon (Gittes et al. 1993), microtubules can resist substantial mechanical deformation, as demonstrated by most microtubules remaining intact after stretch injury (Tang-Schomer et al. 2012). Nonetheless, some microtubules mechanically failed, suggesting that there was a local inability for the microtubules to slide past each other during stretch, leading to rupture. The current data indicates that mechanical vulnerability to dynamic injuries may be increased for smaller axons on average. This has precedence in animal models of TBI, where white matter axons with smaller diameters have been shown to undergo more acute dysfunction, slower recovery of function and/or greater degeneration than large diameter axons (Reeves et al. 2005).

Here, fewer microtubules per axon appears to result in more strain per microtubule, leading to a higher number of undulations and a greater average undulation length for the female axons compared to male axons after TBI. In addition, corresponding to transport interruption due to microtubule damage, there was more extensive accumulation of beta-tubulin in axonal swellings 24 h following injury in female axons compared to male axons. Furthermore, as

found for in vivo TBI models, there also appeared to be functional differences related to size and ultrastructure of stretch injured axons and their ability to generate functional intra-axonal calcium signals.

Pathological calcium influx into axons has long been regarded as an important feature of TAI in animal and in vitro TBI models as well as in human TBI (Fineman et al. 1993; Maxwell et al. 1995; Wolf et al. 2001). While difficult to observe directly in vivo, calcium influx has been nonetheless evident by the protein degradation products of calcium-dependent proteases, shown to accumulate in damaged axons after TBI (Iwata et al. 2004; Saatman et al. 1996). In addition, direct evidence of massive intra-axonal calcium influx following trauma has been characterized in vitro and shown to be a downstream consequence of sodium channel dysregulation (Iwata et al. 2004; Wolf et al. 2001).

Since the extent of calcium influx is linked with the extent of microtubule damage and undulation formation after injury, this represents a negative synergetic effect that can collectively push axons towards degeneration. This appears to be the case in the present study, where female axons displayed more extensive structural and physiological disruption shortly after injury that appears to have pushed them to degenerate at a much greater rate than the male axons. The intra-axonal calcium influx profiles following injury were different for human axons than for rat axons, with human axons 1) experiencing greater calcium influx immediately following injury, which may be due to the larger circumferential area allowing for greater density of calcium related channels, and 2) quickly reducing calcium fluorescence, which may be attributed to tighter calcium regulation in human axons as compared to rat axons.

These data collectively demonstrate that sexual dimorphism down to the nanoscale of axonal architecture can predispose female axons to greater mechanical damage and physiological dysfunction resulting from traumatic axonal injury in vitro. Therefore, these findings support in vivo examination of potential sex differences in the extent of axonal damage in concussion that may be possible in the near future through emerging non-invasive techniques, such as advanced neuroimaging and blood biomarker analyses.

Acknowledgements

We are grateful to the Penn Vector Core facility for providing us with the genetically encoded calcium indicator GCaMP6 and to the Penn Electron Microscopy core facility for TEM processing.

Funding

This work was supported by the Paul G. Allen Family Foundation, National Institutes of Health grants NS092398 (D.H.S), NS038104 (D.H.S), EB021293 (D.H.S and V.B.S), MH110185 (S.A.A) and the US Department of Defense Grant PT110785 (D.H.S).

Abbreviations

TAI	traumatic axonal injury
TBI	traumatic brain injury
TEM	transmission electron microscopy

iPSC	induced pluripotent stem cell
Ngn2	Neurogenin-2

References

Aboitiz F, Scheibel AB, Fisher RS, Zaidel E, 1992 Fiber composition of the human corpus callosum. Brain Res. 598, 143–153. [PubMed: 1486477]

Abrahams S, Fie SM, Patricios J, Posthumus M, September AV, 2014 Risk factors for sports concussion: an evidence-based systematic review. Br. J. Sports Med 48, 91–97. [PubMed: 24052371]

Ahmadzadeh H, Smith DH, Shenoy VB, 2014 Viscoelasticity of tau proteins leads to strain rate-dependent breaking of microtubules during axonal stretch injury: predictions from a mathematical model. Biophys. J 106, 1123–1133. [PubMed: 24606936]

Ahmadzadeh H, Smith DH, Shenoy VB, 2015 Mechanical effects of dynamic binding between tau proteins on microtubules during axonal injury. Biophys. J 109, 2328–2337. [PubMed: 26636944]

Alexander DC, Hubbard PL, Hall MG, Moore EA, Ptito M, Parker GJ, Dyrby TB, 2010 Orientationally invariant indices of axon diameter and density from diffusion MRI. NeuroImage 52, 1374–1389. [PubMed: 20580932]

Bazarian JJ, Atabaki S, 2001 Predicting postconcussion syndrome after minor traumatic brain injury. Acad. Emerg. Med. Off. J. Soc. Acad. Emerg. Med 8, 788–795.

Benson RR, Meda SA, Vasudevan S, Kou Z, Govindarajan KA, Hanks RA, Millis SR, Makki M, Latif Z, Coplin W, Meythaler J, Haacke EM, 2007 Global white matter analysis of diffusion tensor images is predictive of injury severity in traumatic brain injury. J. Neurotrauma 24, 446–459. [PubMed: 17402851]

Blumbergs PC, Scott G, Manavis J, Wainwright H, Simpson DA, McLean AJ, 1994 Staining of amyloid precursor protein to study axonal damage in mild head injury. Lancet 344, 1055–1056. [PubMed: 7523810]

Broshek DK, Kaushik T, Freeman JR, Erlanger D, Webbe F, Barth JT, 2005 Sex differences in outcome following sports-related concussion. J. Neurosurg 102, 856–863. [PubMed: 15926710]

Chen XH, Meaney DF, Xu BN, Nonaka M, McIntosh TK, Wolf JA, Saatman KE, Smith DH, 1999 Evolution of neurofilament subtype accumulation in axons following diffuse brain injury in the pig. J. Neuropathol. Exp. Neurol 58, 588–596. [PubMed: 10374749]

Covassin T, Swanik CB, Sachs ML, 2003 Sex differences and the incidence of concussions among collegiate athletes. J. Athl. Train 38, 238–244. [PubMed: 14608434]

Dekaban AS, 1978 Changes in brain weights during the span of human life: relation of brain weights to body heights and body weights. Ann. Neurol 4, 345–356. [PubMed: 727739]

Espuny-Camacho I, Michelsen KA, Gall D, Linaro D, Hasche A, Bonnefont J, Bali C, Orduz D, Bilheu A, Herpoel A, Lambert N, Gaspard N, Peron S, Schiffmann SN, Giugliano M, Gaillard A, Vanderhaeghen P, 2013 Pyramidal neurons derived from human pluripotent stem cells integrate efficiently into mouse brain circuits in vivo. Neuron 77, 440–456. [PubMed: 23395372]

Fairbanks SL, Vest R, Verma S, Traystman RJ, Herson PS, 2013 Sex stratified neuronal cultures to study ischemic cell death pathways. J. Vis. Exp e50758. [PubMed: 24378980]

Fineman I, Hovda DA, Smith M, Yoshino A, Becker DP, 1993 Concussive brain injury is associated with a prolonged accumulation of calcium: a 45Ca autoradiographic study. Brain Res. 624, 94–102. [PubMed: 8252419]

Gaw CE, Zonfrillo MR, 2016 Emergency department visits for head trauma in the United States. BMC Emerg. Med 16, 5. [PubMed: 26781953]

Gittes F, Mickey B, Nettleton J, Howard J, 1993 Flexural rigidity of microtubules and actin filaments measured from thermal fluctuations in shape. J. Cell Biol 120, 923–934. [PubMed: 8432732]

Gur RC, Turetsky BI, Matsui M, Yan M, Bilker W, Hughett P, Gur RE, 1999 Sex differences in brain gray and white matter in healthy young adults: correlations with cognitive performance. J. Neurosci 19, 4065–4072. [PubMed: 10234034]

Iwata A, Stys PK, Wolf JA, Chen XH, Taylor AG, Meaney DF, Smith DH, 2004 Traumatic axonal injury induces proteolytic cleavage of the voltage-gated sodium channels modulated by tetrodotoxin and protease inhibitors. J. Neurosci 24, 4605–4613. [PubMed: 15140932]

Janmey PA, Euteneuer U, Traub P, Schliwa M, 1991 Viscoelastic properties of vimentin compared with other filamentous biopolymer networks. J. Cell Biol 113, 155–160. [PubMed: 2007620]

Johnson VE, Stewart W, Smith DH, 2013 Axonal pathology in traumatic brain injury. Exp. Neurol 246, 35–43. [PubMed: 22285252]

Lin M, Pedrosa E, Hrabovsky A, Chen J, Puliafito BR, Gilbert SR, Zheng D, Lachman HM, 2016 Integrative transcriptome network analysis of iPSC-derived neurons from schizophrenia and schizoaffective disorder patients with 22q11.2 deletion. BMC Syst. Biol 10, 105. [PubMed: 27846841]

Lu W, Winding M, Lakonishok M, Wildonger J, Gelfand VI, 2016 Microtubulemicrotubule sliding by kinesin-1 is essential for normal cytoplasmic streaming in Drosophila oocytes. Proc. Natl. Acad. Sci. U. S. A 113, E4995–E5004. [PubMed: 27512034]

Mack CM, Boehm GW, Berrebi AS, Denenberg VH, 1995 Sex differences in the distribution of axon types within the genu of the rat corpus callosum. Brain Res. 697, 152–160. [PubMed: 8593571]

Marar M, McIlvain NM, Fields SK, Comstock RD, 2012 Epidemiology of concussions among United States high school athletes in 20 sports. Am. J. Sports Med 40, 747–755. [PubMed: 22287642]

Maxwell WL, McCreath BJ, Graham DI, Gennarelli TA, 1995 Cytochemical evidence for redistribution of membrane pump calcium-ATPase and ecto-Ca-ATPase activity, and calcium influx in myelinated nerve fibres of the optic nerve after stretch injury. J. Neurocytol 24, 925–942. [PubMed: 8719820]

Miyata Y, Hoshi M, Nishida E, Minami Y, Sakai H, 1986 Binding of microtubule-associated protein 2 and tau to the intermediate filament reassembled from neurofilament 70-kDa subunit protein. Its regulation by calmodulin. J. Biol. Chem 261, 13026–13030. [PubMed: 3093477]

Nixon RA, Paskevich PA, Sihag RK, Thayer CY, 1994 Phosphorylation on carboxyl terminus domains of neurofilament proteins in retinal ganglion cell neurons in vivo: influences on regional neurofilament accumulation, interneurofilament spacing, and axon caliber. J. Cell Biol 126, 1031–1046. [PubMed: 7519617]

Ozdogmus O, Cavdar S, Ersoy Y, Ercan F, Uzun I, 2009 A preliminary study, using electron and light-microscopic methods, of axon numbers in the fornix in autopsies of patients with temporal lobe epilepsy. Anat. Sci. Int 84, 2–6. [PubMed: 19214658]

Paus T, Toro R, 2009 Could sex differences in white matter be explained by g ratio? Front. Neuroanat. 3, 14. [PubMed: 19753325]

Pedrosa E, Sandler V, Shah A, Carroll R, Chang C, Rockowitz S, Guo X, Zheng D, Lachman HM, 2011 Development of patient-specific neurons in schizophrenia using induced pluripotent stem cells. J. Neurogenet 25, 88–103. [PubMed: 21797804]

Perrin JS, Herve PY, Leonard G, Perron M, Pike GB, Pitiot A, Richer L, Veillette S, Pausova Z, Paus T, 2008 Growth of white matter in the adolescent brain: role of testosterone and androgen receptor. J. Neurosci 28, 9519–9524. [PubMed: 18799683]

Perrin JS, Leonard G, Perron M, Pike GB, Pitiot A, Richer L, Veillette S, Pausova Z, Paus T, 2009 Sex differences in the growth of white matter during adolescence. NeuroImage 45, 1055–1066. [PubMed: 19349224]

Pesaresi M, Soon-Shiong R, French L, Kaplan DR, Miller FD, Paus T, 2015 Axon diameter and axonal transport: in vivo and in vitro effects of androgens. NeuroImage 115, 191–201. [PubMed: 25956809]

Povlishock JT, Marmarou A, McIntosh T, Trojanowski JQ, Moroi J, 1997 Impact acceleration injury in the rat: evidence for focal axolemmal change and related neurofilament sidearm alteration. J. Neuropathol. Exp. Neurol 56, 347–359. [PubMed: 9100665]

Reeves TM, Phillips LL, Povlishock JT, 2005 Myelinated and unmyelinated axons of the corpus callosum differ in vulnerability and functional recovery following traumatic brain injury. Exp. Neurol 196, 126–137. [PubMed: 16109409]

Reeves TM, Smith TL, Williamson JC, Phillips LL, 2012 Unmyelinated axons show selective rostrocaudal pathology in the corpus callosum after traumatic brain injury. J. Neuropathol. Exp. Neurol 71, 198–210. [PubMed: 22318124]

Saatman KE, Bozyczko-Coyne D, Marcy V, Siman R, McIntosh TK, 1996 Prolonged calpain-mediated spectrin breakdown occurs regionally following experimental brain injury in the rat. J. Neuropathol. Exp. Neurol 55, 850–860. [PubMed: 8965100]

Sendek A, Fuller HR, Hayre NR, Singh RR, Cox DL, 2014 Simulated cytoskeletal collapse via tau degradation. PloS one 9, e104965. [PubMed: 25162587]

Smith DH, Wolf JA, Lusardi TA, Lee VM, Meaney DF, 1999 High tolerance and delayed elastic response of cultured axons to dynamic stretch injury. J. Neurosci 19, 4263–4269. [PubMed: 10341230]

Smith DH, Johnson VE, Stewart W, 2013 Chronic neuropathologies of single and repetitive TBI: substrates of dementia? Nat. Rev. Neurol 9, 211–221. [PubMed: 23458973]

Staal JA, Vickers JC, 2011 Selective vulnerability of non-myelinated axons to stretch injury in an in vitro co-culture system. J. Neurotrauma 28, 841–847. [PubMed: 21235329]

Suresh S, 2007 Biomechanics and biophysics of cancer cells. Acta Biomater. 3, 413–438. [PubMed: 17540628]

Swadlow HA, Waxman SG, Geschwind N, 1980 Small-diameter nonmyelinated axons in the primate corpus callosum. Arch. Neurol 37, 114–115. [PubMed: 6766715]

Tang-Schomer MD, Patel AR, Baas PW, Smith DH, 2010 Mechanical breaking of microtubules in axons during dynamic stretch injury underlies delayed elasticity, microtubule disassembly, and axon degeneration. FASEB J. 24, 1401–1410. [PubMed: 20019243]

Tang-Schomer MD, Johnson VE, Baas PW, Stewart W, Smith DH, 2012 Partial interruption of axonal transport due to microtubule breakage accounts for the formation of periodic varicosities after traumatic axonal injury. Exp. Neurol 233, 364–372. [PubMed: 22079153]

Vorstman JA, Jalali GR, Rappaport EF, Hacker AM, Scott C, Emanuel BS, 2006 MLPA: a rapid, reliable, and sensitive method for detection and analysis of abnormalities of 22q. Hum. Mutat 27, 814–821. [PubMed: 16791841]

Wang SS, Shultz JR, Burish MJ, Harrison KH, Hof PR, Towns LC, Wagers MW, Wyatt KD, 2008 Functional trade-offs in white matter axonal scaling. J. Neurosci 28, 4047–4056. [PubMed: 18400904]

Wegmann S, Scholer J, Bippes CA, Mandelkow E, Muller DJ, 2011 Competing interactions stabilize pro- and anti-aggregant conformations of human Tau. J. Biol. Chem 286, 20512–20524. [PubMed: 21498513]

Wolf JA, Stys PK, Lusardi T, Meaney D, Smith DH, 2001 Traumatic axonal injury induces calcium influx modulated by tetrodotoxin-sensitive sodium channels. J. Neurosci 21, 1923–1930. [PubMed: 11245677]

Yuan A, Rao MV, Veeranna, Nixon RA, 2017 Neurofilaments and Neurofilament proteins in health and disease. Cold Spring Harb. Perspect. Biol 9.

Yuen TJ, Browne KD, Iwata A, Smith DH, 2009 Sodium channelopathy induced by mild axonal trauma worsens outcome after a repeat injury. J. Neurosci. Res 87, 3620–3625. [PubMed: 19565655]

Yuh EL, Mukherjee P, Lingsma HF, Yue JK, Ferguson AR, Gordon WA, Valadka AB, Schnyer DM, Okonkwo DO, Maas AI, Manley GT, Investigators T-T, 2013 Magnetic resonance imaging improves 3-month outcome prediction in mild traumatic brain injury. Ann. Neurol 73, 224–235. [PubMed: 23224915]

Zhang Y, Pak C, Han Y, Ahlenius H, Zhang Z, Chanda S, Marro S, Patzke C, Acuna C, Covy J, Xu W, Yang N, Danko T, Chen L, Wernig M, Sudhof TC, 2013 Rapid single-step induction of functional neurons from human pluripotent stem cells. Neuron 78, 785–798. [PubMed: 23764284]

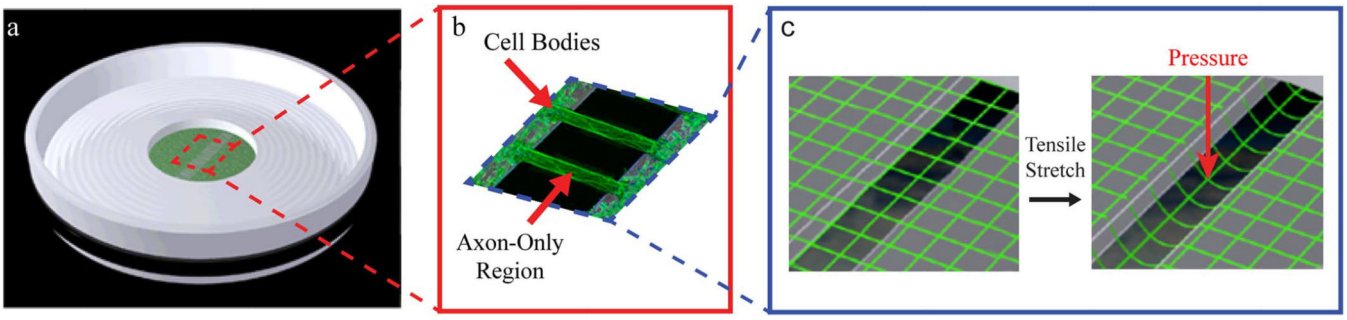

Fig. 1.

In vitro model: dynamic stretch injury of axons.

Pulsed air pressure introduces uniaxial stretch on patterned longitudinally arranged axon tracts, simulating stretch injury of CNS axons during head trauma. (a) The culture well contains a deformable membrane onto which primary cortical neuronal cells are plated. (b) Two separate populations of cells are separated by a lithography fabricated micro-patterned barrier. Axonal processes extend through the 2 mm microchannels to integrate with the opposing population of neurons, thus creating a unique axon-only injury region. (c) Upon controlled delivery of air into a sealed chamber, the subsequent pressure change within the chamber allows the regionally specific deflection of the axon-only region.

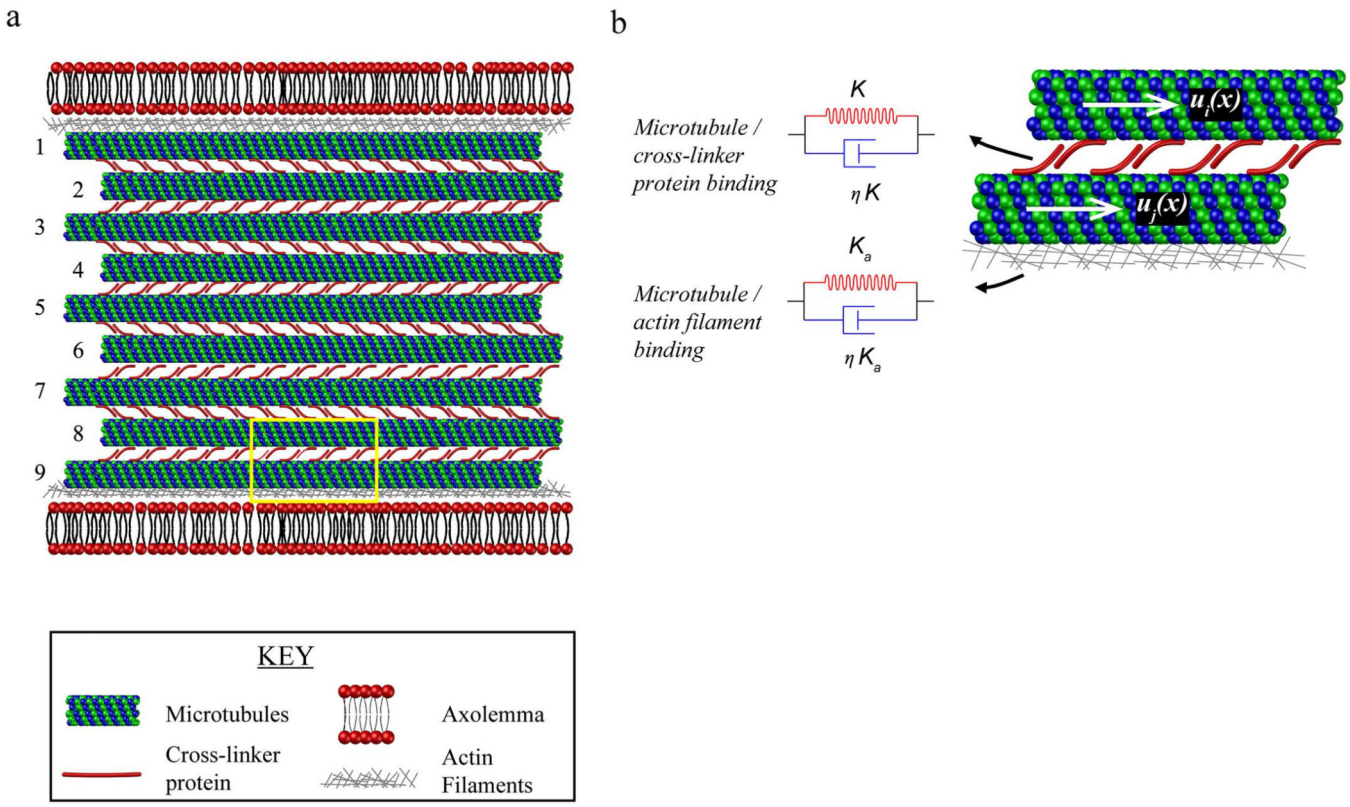

Fig. 2.

Mathematical model of axonal stretch injury for female and male axons. (a) The model incorporates interactions between microtubules, cross-linker proteins, actin filaments and the axolemma. Microtubules are placed in parallel and cross-linked by inverted pairs of cross-linker proteins. Female axons are assumed to have 5 microtubules and male axons 9 microtubules. (b) The binding between microtubules and cross linker proteins and microtubules and actin filaments (highlighted yellow box in (a)), is modeled using a viscoelastic element that consists of a spring and a dashpot. $u_i(x)$ and $u_j(x)$ are the longitudinal displacements in two neighboring microtubules where i and j are between 1 and 5 and 1 and 9 for female and male axons, respectively. (For interpretation of the references to color in this figure legend, the reader is referred to the web version of this article.)

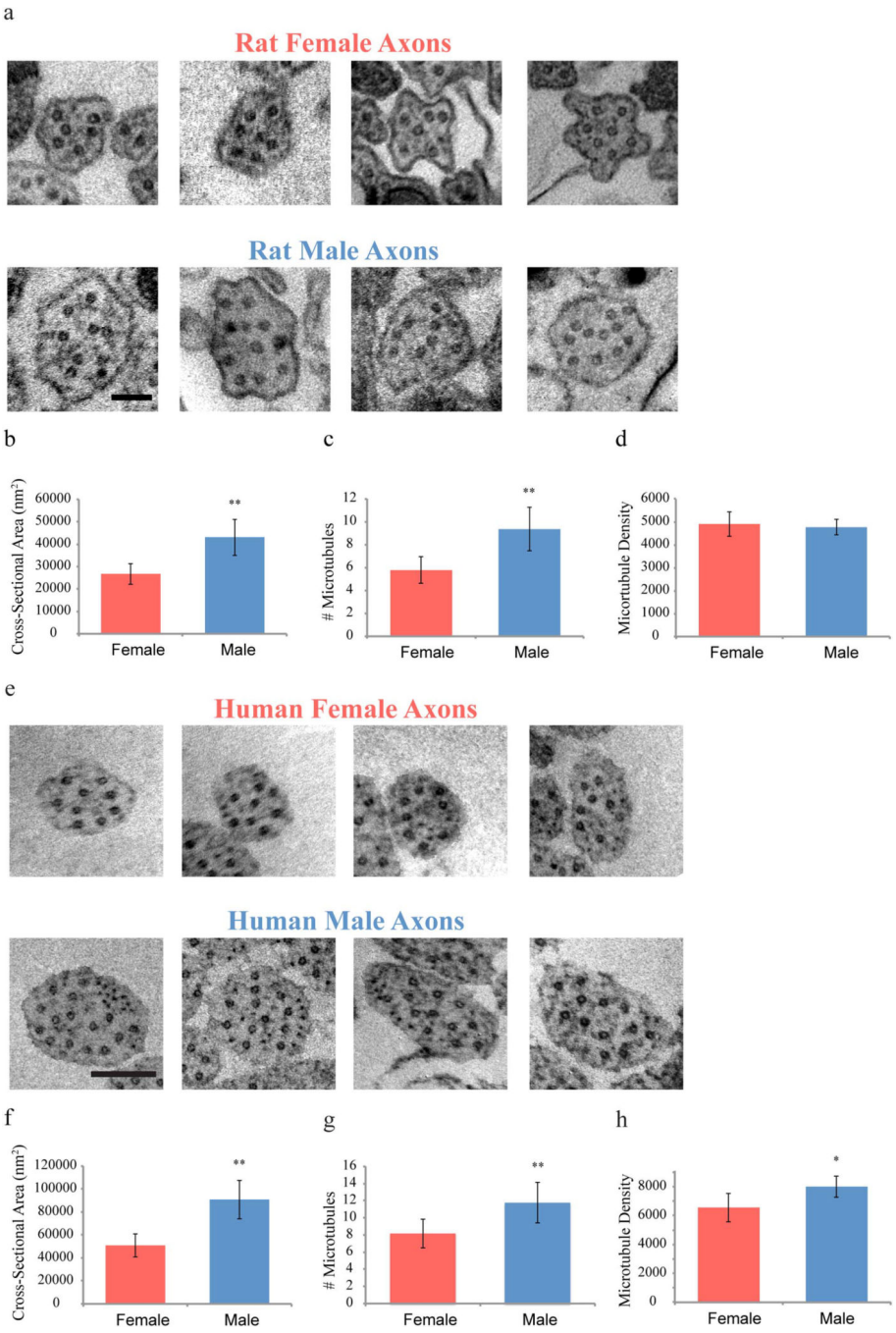

Fig. 3.

Representative electron microscopic examples of cross sectional views of rat and human female and male axons. (a) Male axons are larger with a more complex cytoskeleton than female axons (Scale bar - 100 nm). (b-d) Rat axons were analyzed with regards to cross-sectional area, number of microubules per axon, and microtubule density per axon. (e) A similar sex difference in axonal size and microtubule number is found with human axons (Scale bar - 200 nm). (f–h) Differentiated human iPSC axons were analyzed with

regards to cross-sectional area, number of microubules per axon, and microtubule density per axon.

Data is shown as mean ± s.e.m. ($n = 4$ independent experiments). Statistical significance (*$p < 0.05$, **$p < 0.01$) was evaluated by Students t-test.

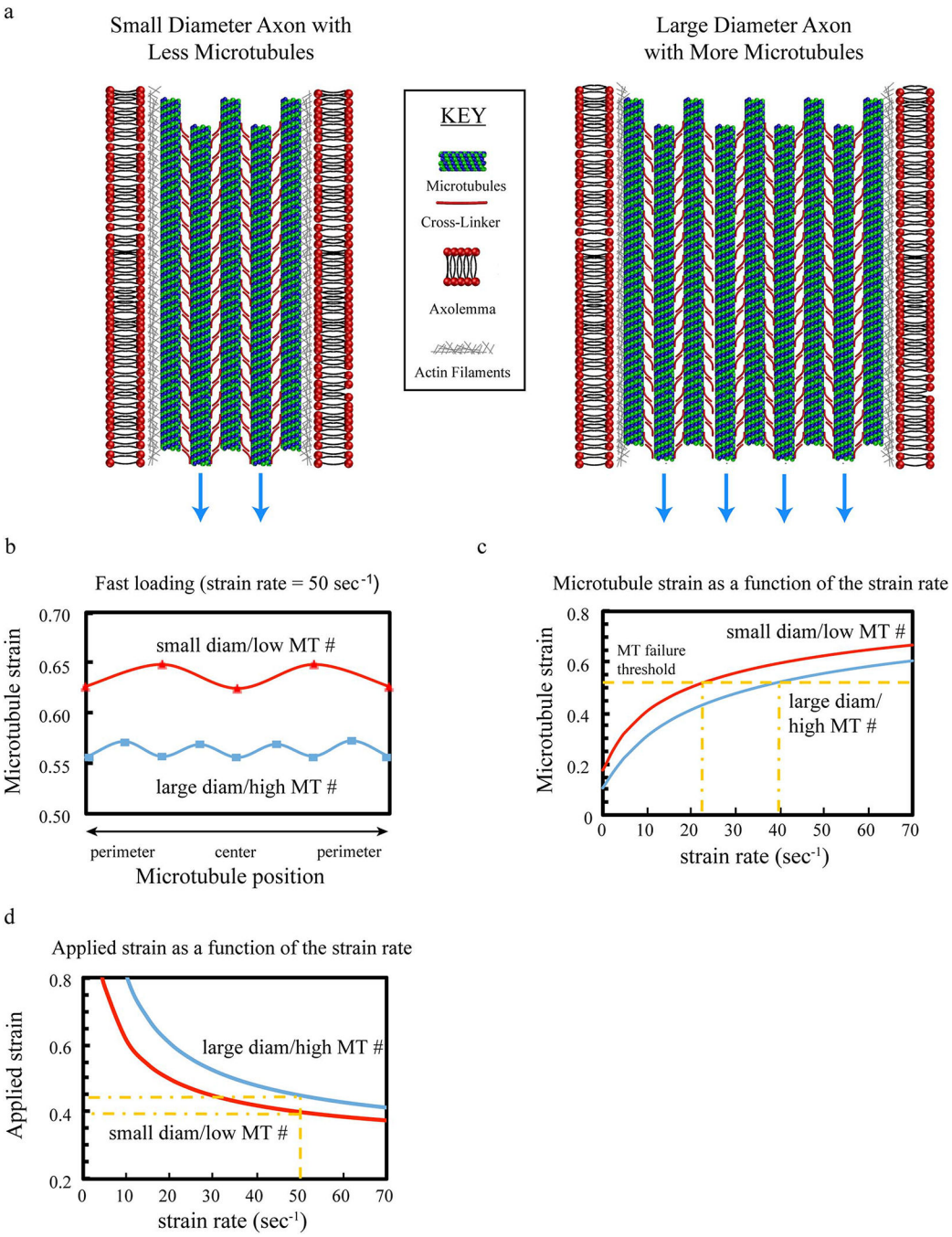

Fig. 4.

Mathematical model of axon stretch injury. (a) The model incorporates the differential size and microtubule number found with TEM, as well as including mechanical associations with cross-linker proteins, actin and the axolemma. (b, c) With the same applied load for both small diameter axons with low microtubule numbers and larger axons with higher numbers of microtubules (blue arrows in a), the stretching relative to microtubule position is greater for smaller diameter axons with lower numbers of microtubules than larger diameter axons with higher numbers of microtubules (b), as is the microtubule strain as a function of strain

rate (c). (d) This causes microtubules in smaller diameter axons with lower numbers of microtubules to fail/rupture at lower levels of strain and strain-rates compared to larger diameter axons with higher numbers of microtubules. (For interpretation of the references to color in this figure legend, the reader is referred to the web version of this article.)

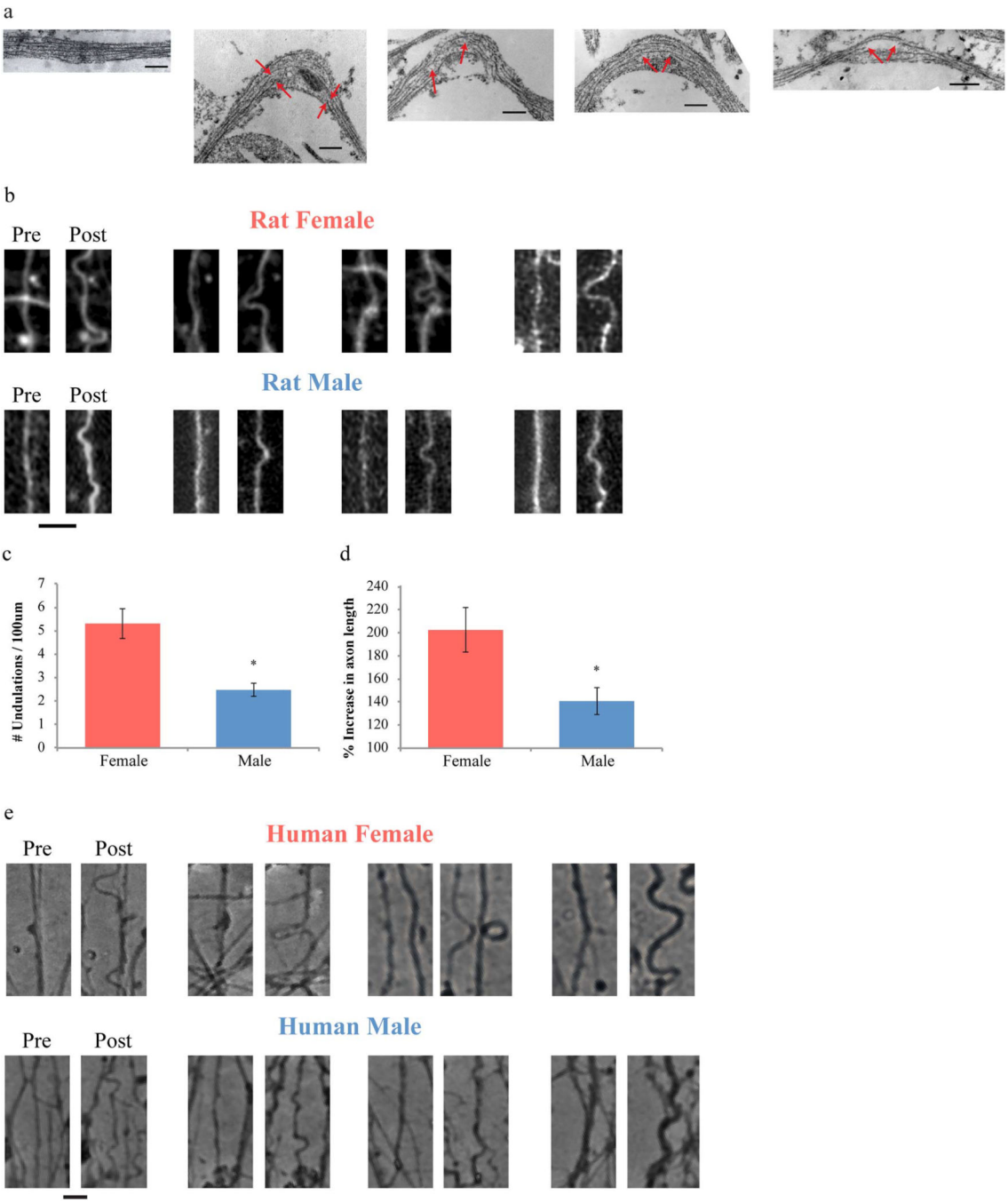

Fig. 5.

Dynamic stretch-injury of axon tracts in vitro. (a) TEM images of axons pre- and post-injury show change of morphology from straight to undulated due to mechanical breaking of microtubules (red arrows depict break sites) (Scale bar, 200 nm). (b) Representative images showing injured female rat axons with more extensive and larger undulation formation compared to male axons (Scale bar - 5 μm), (c, d) Undulations were analyzed with respect to the number of undulations/100 μm (c) and percent increase in axon length (d). (e) The same sex difference was observed for injured human axons (Scale bar - 5 μm). Data is shown as

mean ± s.e.m. (d = 6, e = 7 independent experiments). Statistical significance (* $p < 0.01$) was evaluated by Students t-test. (For interpretation of the references to color in this figure legend, the reader is referred to the web version of this article.)

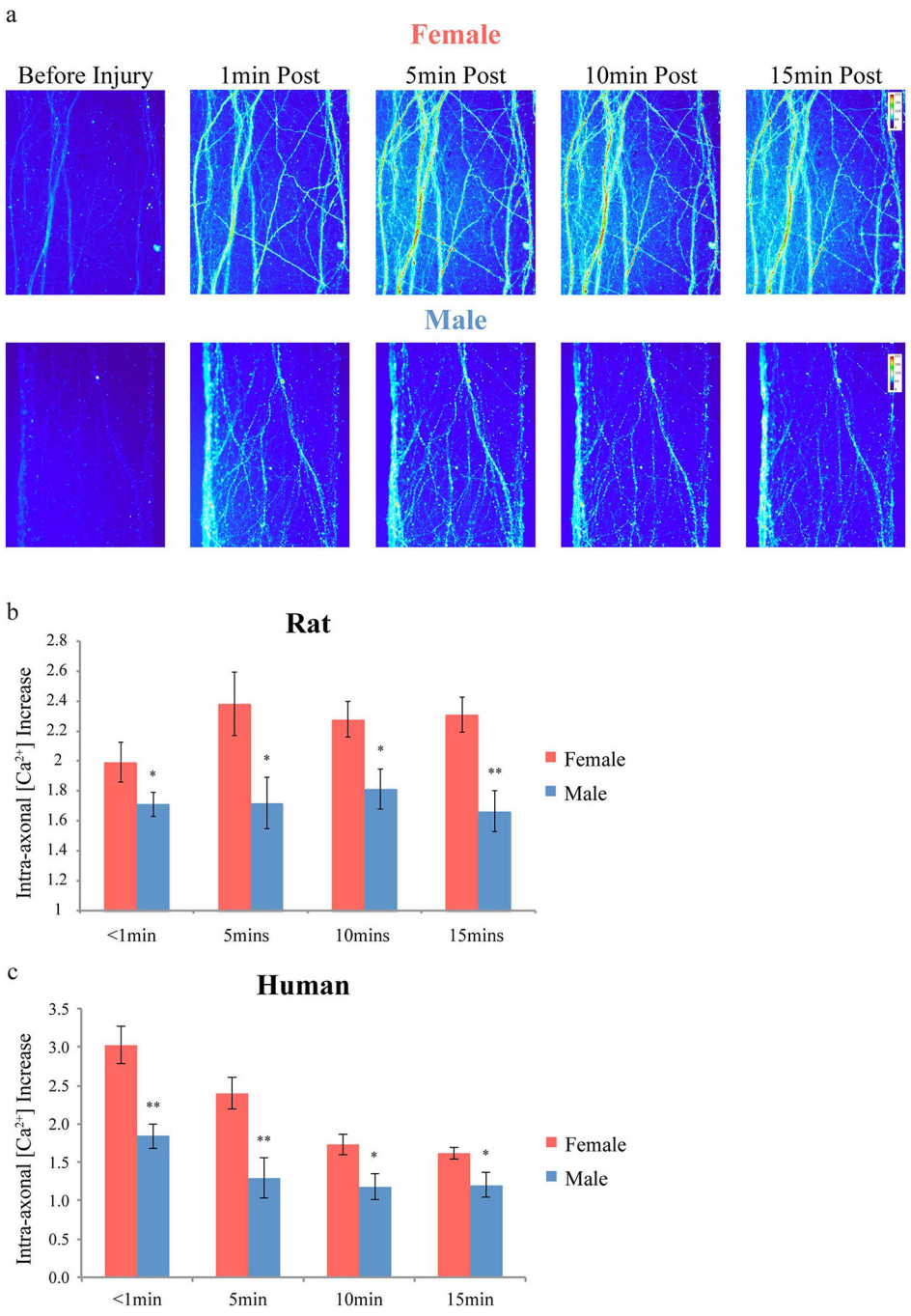

Fig. 6.

Intra-axonal calcium influx following traumatic axonal injury. (a) Representative fluorescent microscopic examples showing greater increases in intra-axonal calcium concentration over 15 min following traumatic axonal injury in female compared to male rat axons. (b, c) This was confirmed by quantification of fluorescence increases post-injury over baseline pre-injury levels for both rat (b) and human axons (c). Data is shown as mean ± s.e.m. (b = 7, c = 4 independent experiments). Statistical significance (*p < 0.05, **p < 0.01) was evaluated by Students t-test.

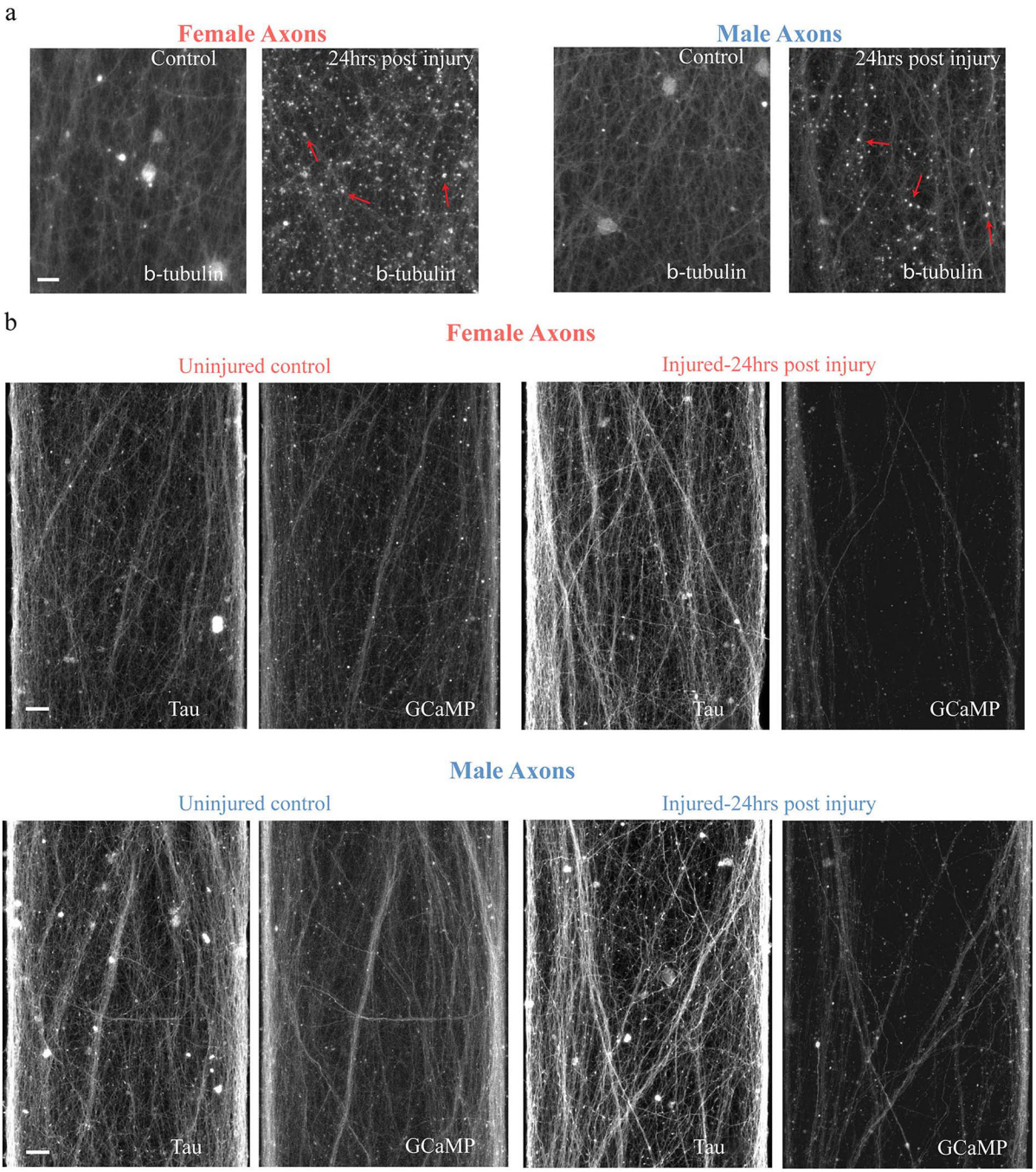

Fig. 7.

Axonal transport interruption and calcium signaling dysfunction. (a) Representative images of rat axons fixed and immunostained for beta-tubulin either uninjured or 24 h following stretch injury, showing female axons with a greater number of transport interruption accumulations than male axons. Red arrows denote examples of axonal beta-tubulin accumulations.

(b) Representative images showing significantly less female axons able to transmit calcium signals 24 h following stretch injury than male axons. Calcium signaling was monitored

using GCaMP6 24 h following injury and compared to total number of axons identified by immunostaining for tau. (For interpretation of the references to color in this figure legend, the reader is referred to the web version of this article.)

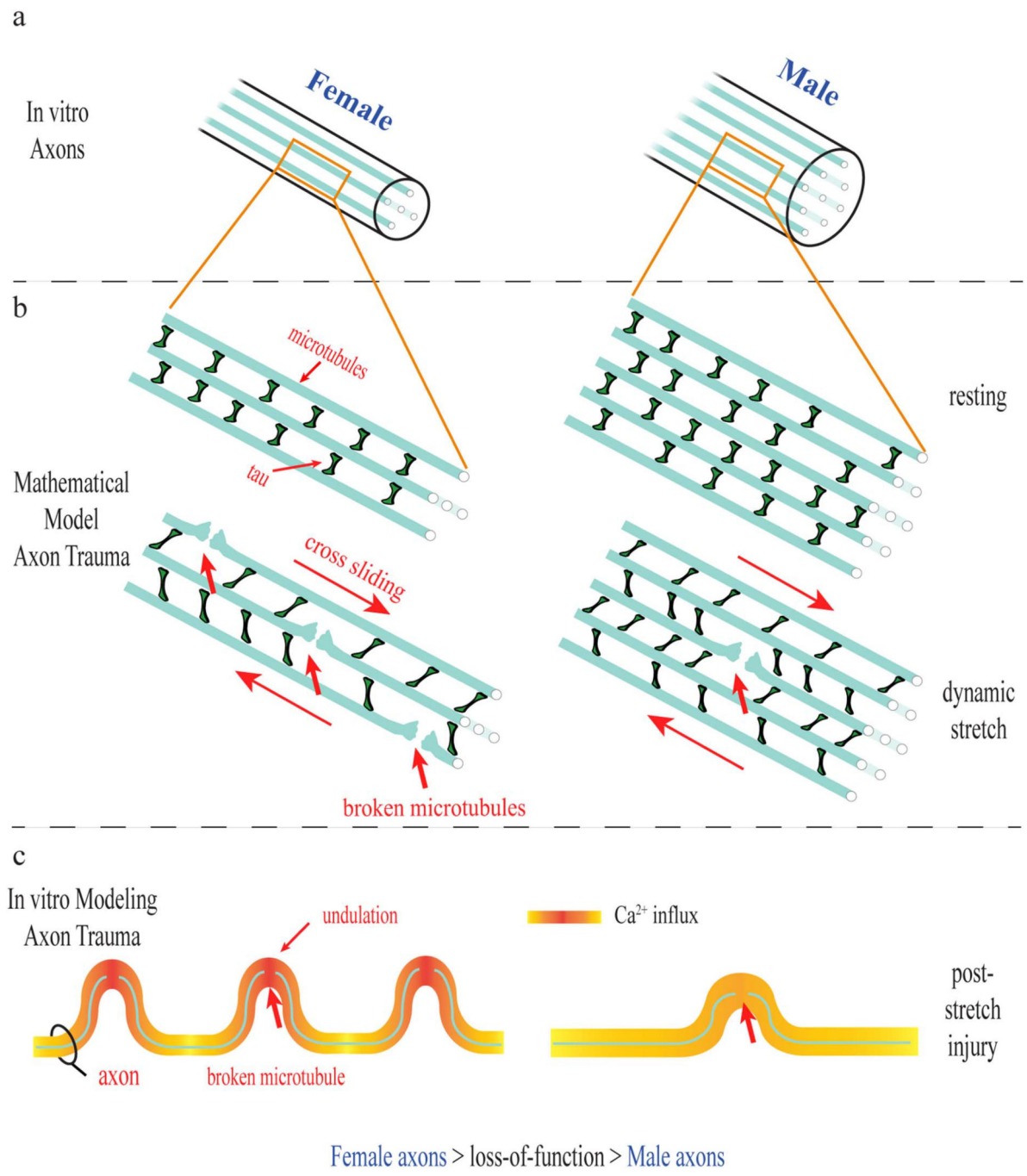

Fig. 8.

Schematic representation of sex-based differences observed in female and male rat and human axons in vitro. (a) Ultrastructural differences in axons were observed with female axons having smaller diameter and less microtubules than male axons. (b) A mathematical model of axon trauma that incorporates the ultrastructural differences demonstrates microtubules in female axons are at greater risk of rupture during trauma given the same applied load. (c) Using an in vitro dynamic stretch injury model, female axons showed larger

undulations, greater calcium influx and greater loss of function than male axons exposed to the same injury.

Table 1

iPSC lines used.

Line	Age	Sex
1BC4	32	Female
2C4	60	Male
3113C4	21	Female
5C4	34	Female
553C2	31	Male
6C4	33	Male
WT1.1	2	Female
WT2.3	3	Male